J. Phys.: Condens. Matter 7 (1995) 7561–7581. Printed in the UK

Excitation spectrum of an antiferromagnetic film with a non-uniform ground state

Leonardo Trallori†, Paolo Politi†, Angelo Rettori† and Maria Gloria Pini‡

† Dipartimento di Fisica dell'Università di Firenze e Sezione INFM di Firenze, Largo E Fermi 2, I-50125 Firenze, Italy

‡ Istituto di Elettronica Quantistica, Consiglio Nazionale delle Ricerche, Via Panciatichi 56/30, I-50127 Firenze, Italy

Received 24 January 1995, in final form 1 May 1995

Abstract. Using a microscopic approach, we study the elementary excitations for a uniaxial antiferromagnetic film with an external magnetic field H applied along the easy axis. For H greater than a critical value, H_S, the system has a non-uniform ground state which is obtained, very rapidly and with high accuracy, in terms of a two-dimensional area preserving map, where the surfaces are introduced as appropriate boundary conditions. The consequent spectrum is calculated in the whole Brillouin zone and the behaviour of the localized surface modes is carefully analysed. It is possible to observe that the lowest-energy modes have substantially a bulk character for low values of $k_\parallel$ (the wavevector in the plane parallel to the surfaces), whilst the localized surface modes have the lowest energy for high values of $k_\parallel$. The relevance of our results for the superlattices composed by ferromagnetic films antiferromagnetically coupled across non-magnetic layers, which present the giant magnetoresistance phenomenon, is discussed, too.

1. Introduction

In recent years much attention has been given to the development of thin magnetic films and the investigation of their properties. For a complete comprehension of these systems, it is essential to determine their elementary excitations that, in the direction normal to the film, are standing waves owing to the absence of translational invariance [1].

Usually, assuming a uniform ground state, in addition to the bulk modes one has different numbers and types of localized surface excitations, characterized by an exponential decay of the amplitude of the spin fluctuations [2, 3]. It is worthwhile to note that, also in the presence of dipolar interaction, the surface modes have lower energies with respect to the volume ones in almost the whole Brillouin zone [4], and consequently they are very important for the thermodynamics.

In a film with some competitive interactions, the lack of translational invariance can produce an inhomogeneous ground state. It should be very interesting to study the properties of the elementary excitations in such a situation, and in particular it is reasonable to expect that the localized surface modes are the most strongly influenced by the non-uniformity of the ground state.

In this paper we present a microscopic study of such a phenomenon in the case of a uniaxial antiferromagnetic film with an external magnetic field H applied along the easy axis and with the spins in each plane belonging to the same sublattice. For the assumed model, it

0953-8984/95/387561+21$19.50

is now well established [5–7] that, owing to the competition between the antiferromagnetic exchange and the magnetic field, one can have an inhomogeneous ground state and low fields can be sufficient to obtain the surface canting. Many different materials can be represented by this model depending on the crystal stucture and the surface orientation: fcc lattices like NiO, MnO, and CoO [8] with (111) surfaces, and bcc lattices such as MnF_2 and FeF_2 [9] with (001) surfaces. However, our analysis presents the greatest relevance for superlattices composed by ferromagnetic films antiferromagnetically coupled across non-magnetic layers, which present the giant magnetoresistance phenomenon [10]. In these systems, parallel and antiparallel configurations are the only ones commonly considered but, on the other hand, all the main experimentally measured quantities are strongly dependent on the spin configuration, so that an exact knowledge of the ground state of the system is of great importance. Moreover, the giant magnetoresistance effect decreases with increasing temperature, as a consequence of a stronger spin mixing for the electrons which is primarily due to the interactions between electrons and spin fluctuations in the magnetic material, and important information on this behaviour can be gained from the excitation spectrum of magnons [11]. Furthermore, it is worthwhile to note that in these systems the non-uniform ground state can be modified through an external parameter, at variance with other systems, like Gd, where the phenomenon of surface magnetic reconstruction is due to the different direction between surface and bulk anisotropies [12].

In an infinitely extended antiferromagnet, it is well known [13] that when H exceeds a critical value, H_{BSF}, a sudden nearly $\pi/2$ rotation of the spin vectors occurs, which drives the system into the so-called bulk spin flop phase. This first-order phase transition is announced by a soft mode for $H = H_{BSF}$ [14].

In the semi-infinite system, assuming an antiferromagnetic ground state with the surface spins antiparallel to H ($AF_{\uparrow\downarrow}$), in addition to the BSF transition, one has that the surface mode softens for $H = H_S \simeq H_{BSF}/\sqrt{2}$ [15, 16]. In this case, the $AF_{\uparrow\downarrow}$ state is only a metastable one for $H < H_S$, while the configuration with the surface spins parallel to H, $AF_{\uparrow\uparrow}$, is the true ground state for $H \leqslant H_{BSF}$. In a previous paper [7], we have argued that for $H = H_S$ the $AF_{\uparrow\downarrow}$ state becomes unstable with respect to the nucleation of a domain wall which interchanges the two sublattices, so that the system evolves, through non-equilibrium configurations, towards the $AF_{\uparrow\uparrow}$ ground state. This description holds for systems in which the uniaxial anisotropy is much lower than the exchange. In such a situation the surface spin flop phase predicted earlier in the literature [17, 18] does not exist [7]. When the two quantities are instead comparable, the domain wall is very narrow and non-uniform metastable states due to the discreteness of the lattice can arise [19].

For a film with a finite number of planes, N, one has two surface modes, localized at the two surfaces, and two different possibilities arise.

For a film with odd N, the situation is analogous to the semi-infinite system: the excitations calculated with respect to the AF state with the spins on both surfaces parallel to the field (ground state) are unstable only at $H \simeq H_{BSF}$, as we will show in the following, while an instability at $H \simeq H_S$ is found if H is reversed, as it was shown by LePage and Camley [20].

For a film with even N, starting from the antiferromagnetic configuration, for $H = H_S$ one observes a complete softening only for the surface mode localized at the surface with the spins antiparallel to the field. Obviously, because of the complete symmetry between the two sublattices, no interchange can occur, so that for $H > H_S$ the system undergoes a phase transition to a non-uniform ground state.

Again, a marked difference exists between the case in which the anisotropy is much lower than the exchange and the one of comparable quantities. In the first situation the

non-uniform configuration is always symmetric with respect to the middle of the sample [7], while in the second one surface-localized canted configurations can arise [6, 19, 21, 22].

In this paper we will concentrate on the low-anisotropy case for a film with even N.

In order to calculate the excitation spectrum in an accurate way, the new ground state must be determined with great precision. In a very recent paper [7] we have shown that this problem can be formulated as a two-dimensional area preserving map [23–25], where the surfaces are introduced with appropriate boundary conditions [26]. In this way, the non-uniform ground state is obtained very rapidly and with high accuracy, and the excitation spectrum can be calculated. Such a high precision turns out to be necessary in order to obtain correctly the spectrum of excitations in the low-energy limit, and in particular the zero-frequency Goldstone mode.

In the non-uniform ground state situation, our most interesting results are the following ones:

- many modes show a hybridization phenomenon;
- the localized surface modes are not the lowest-energy ones for low values of $k_{\parallel}$, but they do become the lowest-energy modes on increasing of the wavevector, by means of successive hybridizations.

A similar study was previously performed by Nörtemann *et al* and Camley and Stamps [27, 28], but they investigated a model where the uniaxial anisotropy is absent, and they only analysed the H dependence of the gap in the spectrum of the excitations and the behaviour of the eigenfunctions for a fixed value of the wavevector.

The layout of the paper is as follows. In section 2 the model is introduced and, for the sake of completeness, the method to determine the ground state in the mean-field approximation is briefly reported, too. The formal treatment for obtaining the excitation spectrum is developed in section 3, and the results obtained starting with a uniform and a non-uniform ground state are reported in sections 4 and 5, respectively. Finally, in section 6 the conclusions are summarized.

2. The model and the ground state

We want to describe a bcc two-sublattice Heisenberg antiferromagnet with nearest-neighbour exchange interaction. We consider a film with an even number of planes, N, and (100) surfaces, so that the first plane belongs to the A sublattice, while the last one belongs to the B sublattice (see figure 1). In order to consider the excitations of the superlattice structure we will confine our attention to the limit where the ferromagnetic films can be regarded as very thin, so that each of them will be associated with a single plane of the antiferromagnetic film structure. Moreover, we will suppose the spins belonging to a given ferromagnetic film to be linked together by a very strong intrafilm exchange. The Hamiltonian is thus given by

$$\mathcal{H} = -H\left[\sum_b S_b^z + \sum_a S_a^z\right] - K\left[\sum_b (S_b^z)^2 + \sum_a (S_a^z)^2\right] + J\sum_a\sum_\delta S_a \cdot S_{a+\delta} - \frac{J_0}{2}\left[\sum_a\sum_{\delta_0} S_a \cdot S_{a+\delta_0} + \sum_b\sum_{\delta_0} S_b \cdot S_{b+\delta_0}\right] \tag{1}$$

where $J > 0$, $K > 0$ are the exchange interaction and the single-ion uniaxial anisotropy, respectively, and $J_0 > 0$ denotes the intralayer ferromagnetic exchange interaction which is present only when the superlattice structure is considered, whilst it is set equal to zero

in the antiferromagnetic film case. δ denotes the vectors connecting an A spin to its z nearest-neighbour B spins: $a + \delta = b$ ($z = 8$); δ_0 denotes the two-dimensional vectors connecting a spin to its z_0 next-nearest neighbours belonging to the same plane ($z_0 = 4$). In the following we will present extensive results for the antiferromagnetic film (i.e. for $J_0 = 0$) and we will then show the effect of the intralayer ferromagnetic exchange.

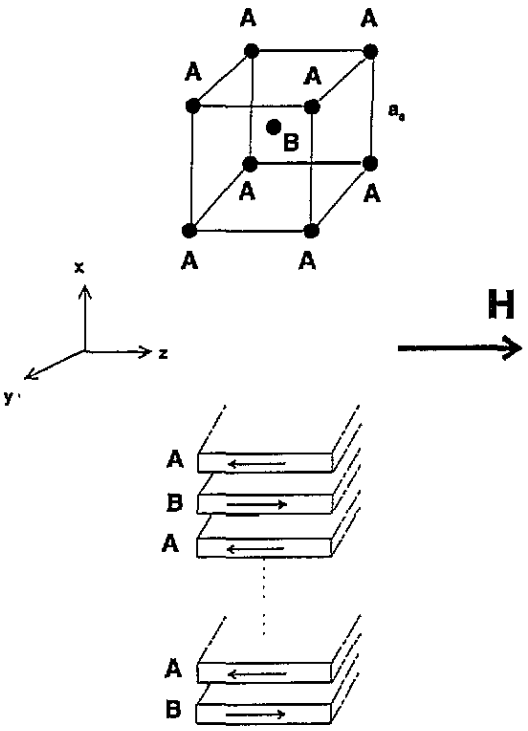

Figure 1. Lattice and magnetic structure of the considered system.

We choose the x axis perpendicular to the surfaces, while the yz plane is the film plane (see figure 1). It will be useful to introduce an index $n = 1, 2, \ldots, N$ to enumerate the different planes, so that

$$a_x = 2(n-1)\frac{a_0}{2} \tag{2a}$$

$$b_x = (2n-1)\frac{a_0}{2} \tag{2b}$$

$$\delta_x = \delta_n \frac{a_0}{2} \qquad (\delta_n = \pm 1) \tag{2c}$$

and in the following we will always put $a_0 = 1$. We decompose each vector into its yz and x components. For example:

$$a = (a_\parallel, a_x) \tag{3}$$

and it is clear that the x component is fully specified by the plane index n.

For the determination of the ground state we assume that all the spins belonging to the same plane are ferromagnetically aligned. In this way the energy for a film with N planes reduces to the energy of an N-spin chain:

$$\frac{E}{N_\parallel S} = H_E \sum_{n=2}^{N} \cos(\phi_n - \phi_{n-1}) - \sum_{n=1}^{N} [H_A \cos^2 \phi_n + 2H \cos \phi_n] \tag{4}$$

with $H_E = zJS$, $H_A = 2KS$. In the following we will always adopt $H_E = 100$ kG and $H_A = 0.9$ kG, so that we have $H_{BSF} \equiv \sqrt{2H_AH_E + H_A^2} = 13.45$ kG and $H_S \equiv \sqrt{H_AH_E + H_A^2} = 9.53$ kG. (We have put $g\mu_B = 1$, so that the energies will be measured in kG.)

The equilibrium configurations are obtained by derivation with respect to the angles ϕ_n:

$$(1 - \delta_{N,n})\sin(\phi_{n+1} - \phi_n) + (1 - \delta_{1,n})\sin(\phi_{n-1} - \phi_n) + 2\frac{H}{H_E}\sin\phi_n + \frac{H_A}{H_E}\sin 2\phi_n = 0 \quad (5)$$

with $n = 1, \ldots, N$.

Defining $s_n = \sin(\phi_n - \phi_{n-1})$, the previous equations can be written, for $n = 2, \ldots, N-1$, as a two-dimensional mapping

$$\phi_{n+1} = \phi_n + \sin^{-1}(s_{n+1}) \quad (6a)$$

$$s_{n+1} = s_n - 2\frac{H}{H_E}\sin\phi_n - \frac{H_A}{H_E}\sin 2\phi_n \quad (6b)$$

and the terms with the Kronecker δ, which represent the presence of surfaces, are taken into account, introducing two fictitious planes $n = 0$ and $n = N + 1$, so that we have the following boundary conditions:

$$s_1 = \sin(\phi_1 - \phi_0) = 0 \quad (7a)$$

$$s_{N+1} = \sin(\phi_{N+1} - \phi_N) = 0. \quad (7b)$$

Among all the trajectories obtained from (6), which are the same as those of the infinitely extended system, the physical ones, representing equilibrium configurations for the film, must have two intersections with the $s = 0$ axis separated by exactly N steps of the recursive mapping: a very selective condition. Of course if more trajectories satisfy these conditions, the ground state is that one which is stable with respect to spin wave excitations and has the lowest energy.

For $H < H_S'$ (which is a value slightly lower than H_S because of the metastability region associated with the first-order nature of the phase transition the system undergoes [14]), the ground state for the film is the usual antiferromagnetic one, represented by the fixed points $P_{\pm}^{AF}$ (that is $(-\pi, 0)$ and $(0, 0)$).This configuration always satisfies the boundary conditions (7), but, for $H > H_S$, it cannot be a minimum for the system, since it turns out to be unstable with respect to a linear spin wave analysis. So, there must be other equilibrium configurations representing the ground state. In fact, in this case, we have non-homotopic to zero curves that cross the $s = 0$ line in two different points. For any fixed N one and only one among these curves satisfies the corresponding boundary conditions. The associated spin configuration is stable and its energy is smaller than the antiferromagnetic one and thus we obtain the new, non-uniform ground state. In figure 2 we report the phase portrait for $H_S < H < H_{BSF}$ with the non-homotopic to zero curves giving the ground state for different values of N. The corresponding spin configurations are reported in figure 3. For sufficiently thick films, the spins on the two surfaces tend to be aligned with H producing, close to the surfaces, two nearly antiferromagnetic regions which are separated by a domain wall in the middle of the sample.

For $H > H_{BSF}$ the phase portraits and the ground state configurations are shown in figure 4 and figure 5 respectively. We note that, for thick films, the spins in the middle region present the typical bulk spin flop configuration, represented by the $P_{\pm}^{BSF}$ fixed points (that is $(\pm\overline{\phi}, \pm\sin 2\overline{\phi})$, where $\cos\overline{\phi} = H/(2H_E - H_A)$).

So, both for H smaller and larger than H_{BSF}, a large part of the spin configuration is nearly uniform. This occurs close to the surfaces at low fields and in the interior at

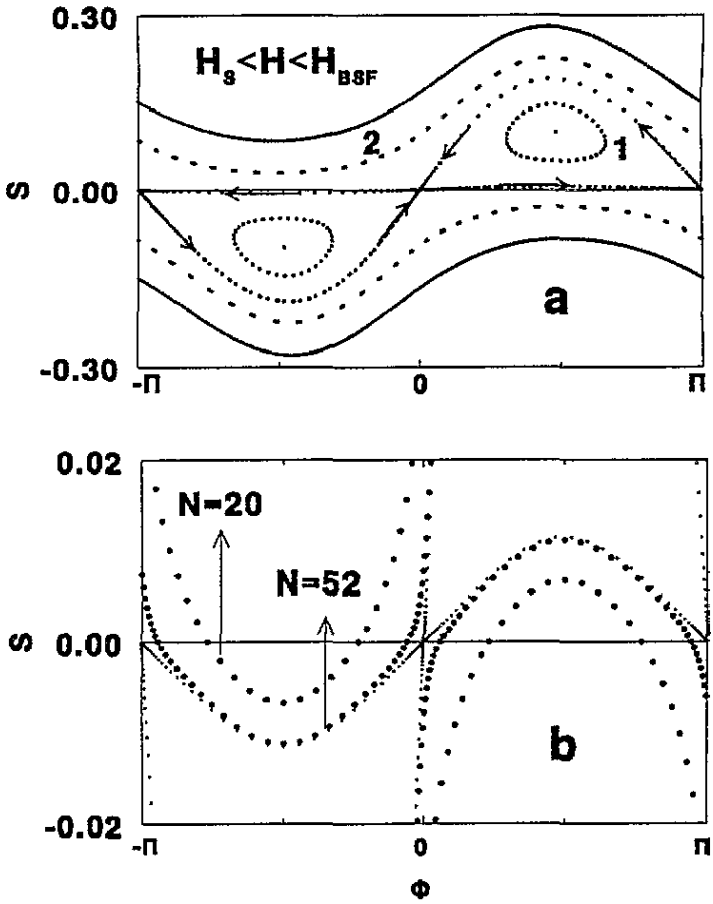

Figure 2. Phase portrait obtained from mapping (6), for $H = 10$ kG. (a) The inflowing and outflowing orbits (denoted by the arrows) associated with the hyperbolic fixed points, elliptic orbits (1) encircling the homonimous fixed points, and non-homotopic to zero curves (2) are shown. (b) Enlargement of (a) around the $s = 0$ axis. The non-homotopic to zero curves providing the ground state configuration for a $N = 52$-plane film and a $N = 20$ one are reported.

higher fields. This is due to the different location of the $P_{\pm}^{AF}$ and $P_{\pm}^{BSF}$ fixed points and to their different nature for low and high field. A uniform configuration corresponds to many steps of the map in proximity to the hyperbolic fixed point. For $H < H^{BSF}$, the $P_{\pm}^{AF}$ are hyperbolic and they lie on the boundary condition line, so that the uniform region takes place close to the surface. In contrast, for $H > H^{BSF}$, the $P_{\pm}^{BSF}$ are hyperbolic but they do not belong to the $s = 0$ axis, so that a surface canting must be present before reaching the bulk spin flop phase in the middle of the sample. In this sense, a surface magnetic reconstruction is present only for $H \geqslant H_{BSF}$.

3. Elementary excitations: general treatment

In this section we determine the dynamical matrix which must be diagonalized in order to obtain the dispersion curves of the excitations and their relative eigenvectors. Taking

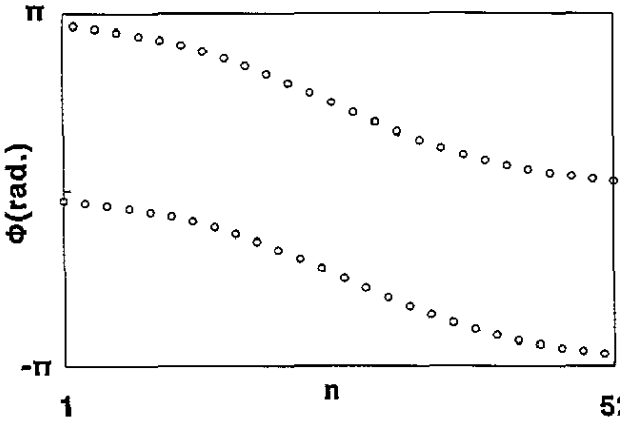

Figure 3. Ground state configuration for a $N = 52$-plane film for $H = 10$ kG.

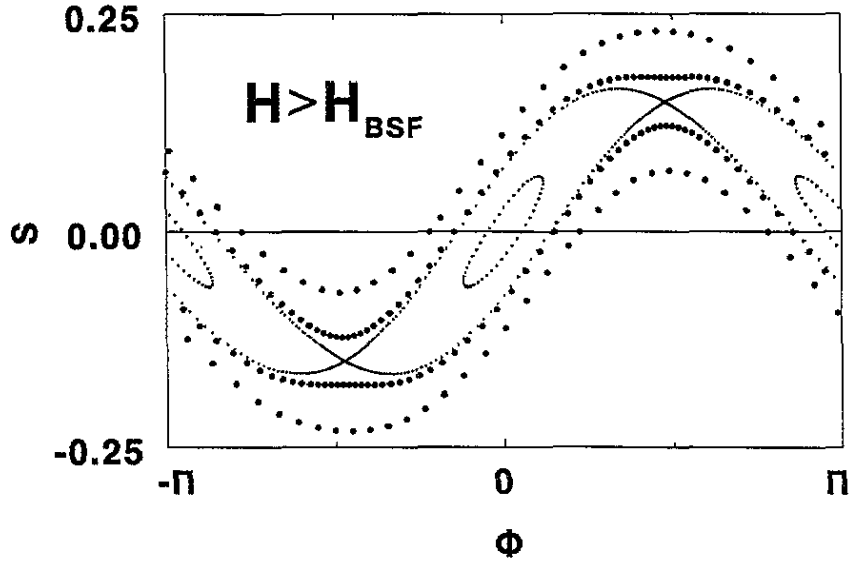

Figure 4. Phase portrait obtained from mapping (6) for $H = 15$ kG. The AF and BSF fixed points have interchanged their character with respect to figure 2. Again, the non-homotopic to zero curves providing the ground state configuration for a $N = 52$-plane film and a $N = 20$ one are reported.

into account that in the general case each plane has a characteristic canting angle we must introduce a local reference frame $(\overline{x}, \overline{y}, \overline{z})$ so that the spin components can be written as:

$$S_a^x = S_a^{\overline{x}} \tag{8a}$$

$$S_a^y = S_a^{\overline{y}} \cos\theta_{2n-1} + S_a^{\overline{z}} \sin\theta_{2n-1} \tag{8b}$$

$$S_a^z = S_a^{\overline{z}} \cos\theta_{2n-1} - S_a^{\overline{y}} \sin\theta_{2n-1} \tag{8c}$$

$$S_b^x = S_b^{\overline{x}} \tag{8d}$$

$$S_b^y = S_b^{\overline{y}} \cos\theta_{2n} + S_b^{\overline{z}} \sin\theta_{2n} \tag{8e}$$

$$S_b^z = S_b^{\overline{z}} \cos\theta_{2n} - S_b^{\overline{y}} \sin\theta_{2n} \tag{8f}$$

where θ is the angle the spins in each layer form with the direction of the applied field, and n runs now from one to $N/2$.

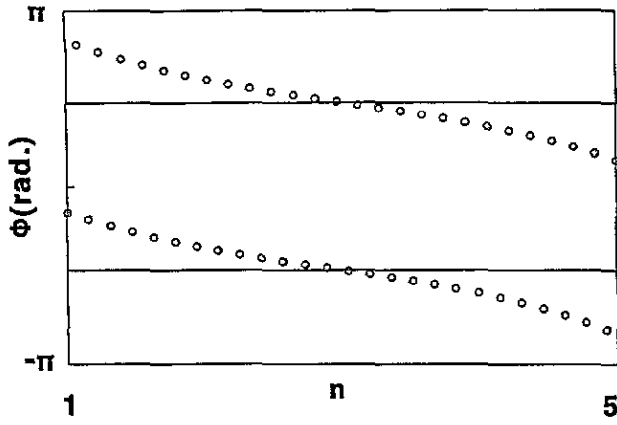

Figure 5. Ground state configuration for a $N = 52$-plane film for $H = 15$ kG. *The solid horizontal lines refer to the* uniform bulk spin flop configuration of the infinite system for the same value of the magnetic field.

Introducing the operators

$$\mathcal{S}^{\pm}_{a(b)} = \mathcal{S}^{x}_{a(b)} \pm \mathcal{S}^{y}_{a(b)} \tag{9}$$

and performing a Fourier analysis in the yz plane (where the system maintains translational invariance), so that

$$\mathcal{S}^{\pm}_{a} = \frac{1}{\sqrt{N}} \sum_{k_\parallel} \exp(\pm i k_\parallel \cdot a_\parallel) \mathcal{S}^{\pm}_{A}(k_\parallel, n, t) \tag{10}$$

$$\mathcal{S}^{\pm}_{b} = \frac{1}{\sqrt{N}} \sum_{k_\parallel} \exp(\mp i k_\parallel \cdot b_\parallel) \mathcal{S}^{\pm}_{B}(k_\parallel, n, t) \tag{11}$$

the linearized Hamiltonian is given by

$$\begin{aligned}
2S\mathcal{H} = {} & \sum_{k_\parallel} \sum_{n=1}^{\frac{N}{2}} \sum_{n'=1}^{\frac{N}{2}} T^{11}_{n,n'} \mathcal{S}^{-}_{A}(k_\parallel, n', t) \mathcal{S}^{+}_{A}(k_\parallel, n, t) \\
& + \sum_{k_\parallel} \sum_{n=1}^{\frac{N}{2}} \sum_{n'=1}^{\frac{N}{2}} \frac{1}{2} T^{13}_{n,n'} [\mathcal{S}^{+}_{A}(k_\parallel, n', t) \mathcal{S}^{+}_{A}(k_\parallel, n, t) + \mathcal{S}^{-}_{A}(k_\parallel, n', t) \mathcal{S}^{-}_{A}(k_\parallel, n, t)] \\
& + \sum_{k_\parallel} \sum_{n=1}^{\frac{N}{2}} \sum_{n'=1}^{\frac{N}{2}} T^{22}_{n,n'} \mathcal{S}^{-}_{B}(k_\parallel, n', t) \mathcal{S}^{+}_{B}(k_\parallel, n, t) \\
& + \sum_{k_\parallel} \sum_{n=1}^{\frac{N}{2}} \sum_{n'=1}^{\frac{N}{2}} \frac{1}{2} T^{24}_{n,n'} [\mathcal{S}^{+}_{B}(k_\parallel, n', t) \mathcal{S}^{+}_{B}(k_\parallel, n, t) + \mathcal{S}^{-}_{B}(k_\parallel, n', t) \mathcal{S}^{-}_{B}(k_\parallel, n, t)] \\
& + \sum_{k_\parallel} \sum_{n=1}^{\frac{N}{2}} \sum_{n'=1}^{\frac{N}{2}} T^{12}_{n,n'} [\mathcal{S}^{+}_{A}(k_\parallel, n', t) \mathcal{S}^{+}_{B}(k_\parallel, n, t) + \mathcal{S}^{-}_{A}(k_\parallel, n', t) \mathcal{S}^{-}_{B}(k_\parallel, n, t)] \\
& + \sum_{k_\parallel} \sum_{n=1}^{\frac{N}{2}} \sum_{n'=1}^{\frac{N}{2}} T^{14}_{n,n'} [\mathcal{S}^{+}_{A}(k_\parallel, n', t) \mathcal{S}^{-}_{B}(k_\parallel, n, t) + \mathcal{S}^{-}_{A}(k_\parallel, n', t) \mathcal{S}^{+}_{B}(k_\parallel, n, t)]
\end{aligned} \tag{12}$$

where the explicit expression for the $(N/2 \times N/2)$ matrix T^{ij} is reported in the appendix.

From the equation of motion in the Heisenberg representation ($\hbar = 1$):

$$i\frac{d}{dt}\mathcal{S}^{\pm}_{A(B)} = [\mathcal{S}^{\pm}_{A(B)}, \mathcal{H}] \tag{13}$$

and assuming a plane-wave-like time dependence

$$\mathcal{S}^{\pm}_{A(B)}(k_{\parallel}, n, t) = \exp(-iEt)\mathcal{S}^{\pm}_{A(B)}(k_{\parallel}, n) \tag{14}$$

we obtain for the linearized equation of motion

$$\begin{bmatrix} T^{11} & T^{12} & T^{13} & T^{14} \\ -(T^{12})^{T} & -T^{22} & -(T^{14})^{T} & -T^{24} \\ -T^{13} & -T^{14} & -T^{11} & -T^{12} \\ (T^{14})^{T} & T^{24} & (T^{12})^{T} & T^{22} \end{bmatrix} \begin{bmatrix} \mathcal{S}^{+}_{A} \\ \mathcal{S}^{+}_{B} \\ \mathcal{S}^{-}_{A} \\ \mathcal{S}^{+}_{B} \end{bmatrix} = E \begin{bmatrix} \mathcal{S}^{+}_{A} \\ \mathcal{S}^{-}_{B} \\ \mathcal{S}^{-}_{A} \\ \mathcal{S}^{+}_{B} \end{bmatrix} \tag{15}$$

which can be rewritten as an eigenvalue equation in terms of the $(2N \times 2N)$ T matrix

$$TS = ES. \tag{16}$$

For a film with N planes we have N positive and N negative eigenvalues. Because T is real and non-symmetric it is necessary to distinguish between right (S_R) and left (S_L) eigenvectors

$$TS_R = ES_R \tag{17}$$

$$S_L T = ES_L \tag{18}$$

so that the normalization factor turns out to be

$$c^2 = [S_L(T, E)] \times [S_R(T, E)] = [S_R(T^{T}, E)]^{T} \times [S_R(T, E)]. \tag{19}$$

In the following we will consider only the positive eigenvalues. However the negative ones are fundamental in order to obtain the correct zero-point contribution to the thermodynamical properties, like the $T = 0$ spin reduction [3, 29].

4. Elementary excitations: uniform ground state

With a uniform AF ground state we have

$$\theta_{2n-1} = \pi \ \forall n \tag{20a}$$

$$\theta_{2n} = 0 \ \forall n \tag{20b}$$

so that the expressions for the T^{ij} matrices become much simpler:

$$T^{11}_{n,n'} = [-H + 2KS + (zJS/2)(1 + (1 - \delta_{n,1})) + z_0 J_0 S(1 - \gamma_0(k_{\parallel}))]\delta_{n,n'} \tag{21a}$$

$$T^{22}_{n,n'} = [+H + 2KS + (zJS/2)(1 + (1 - \delta_{n,N/2})) + z_0 J_0 S(1 - \gamma_0(k_{\parallel}))]\delta_{n,n'} \tag{21b}$$

$$T^{12}_{n,n'} = zJS\gamma(k_{\parallel})\delta_{2n-1+\delta_n,2n'} \tag{21c}$$

$$T^{13}_{n,n'} = T^{24}_{n,n'} = T^{14}_{n,n'} = 0. \tag{21d}$$

Going back to the absolute reference frame, we have two separate systems of equations for the $S^{\pm}$ operators:

$$\begin{bmatrix} T^{11} & T^{12} \\ -(T^{12})^{T} & -T^{22} \end{bmatrix} \begin{bmatrix} S^{+}_{A} \\ S^{+}_{B} \end{bmatrix} = E \begin{bmatrix} S^{+}_{A} \\ S^{+}_{B} \end{bmatrix} \tag{22}$$

$$\begin{bmatrix} -T^{11} & -T^{12} \\ (T^{12})^{T} & T^{22} \end{bmatrix} \begin{bmatrix} S^{-}_{A} \\ S^{-}_{B} \end{bmatrix} = E \begin{bmatrix} S^{-}_{A} \\ S^{-}_{B} \end{bmatrix}. \tag{23}$$

In fact, owing to the rotational invariance in the yz plane, the eigenvector components S^{+} and S^{-} are completely decoupled and they differ only by a phase factor $\Delta\phi = \pi$. Consequently, the excitations have a circular polarization [4] and it is sufficient to specify only one component.

• $H = 0$, $J_0 = 0$. We have $N/2$ eigenvalues which are doubly degenerate owing to the perfect equivalence of the two sublattices. In figure 6 we report the dispersion curves obtained for a $N = 52$-plane film. The lowest curve corresponds to the two surface modes, each of them localized close to *only* one surface, as is evident from figure 7(a,b) where the respective eigenvectors are reported, respectively for $k_\parallel = 0$ and $k_\parallel = (\pi/4, \pi/4)$. With the growing of $k_\parallel$ the localization increases, because—as will be clearer later on—adjacent planes are less coupled. At $k_\parallel = 0$, the localization is entirely due to the anisotropy (i.e. there is a complete delocalization if $H_A = 0$).

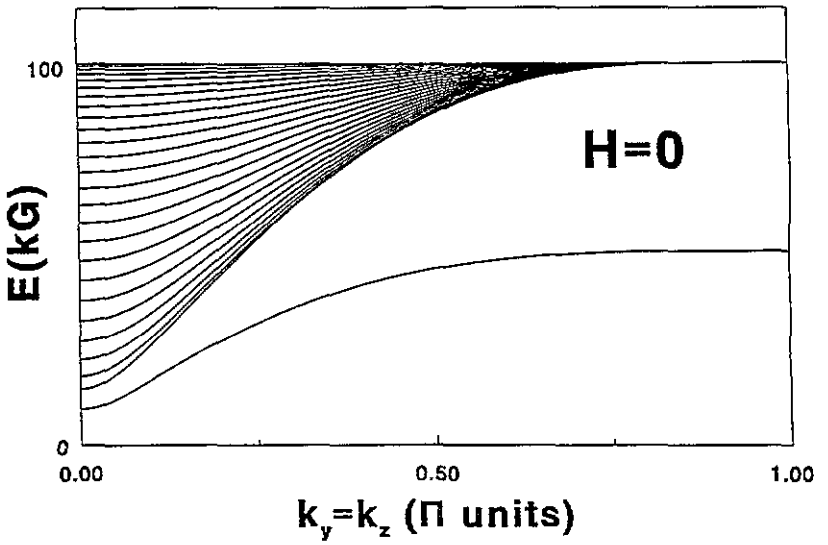

Figure 6. The energy spectrum for a $N = 52$-plane film for $H = 0$. Each line is doubly degenerate. The lowest curve refers to the two degenerate surface modes.

The log plot of figure 7(c) clearly shows the exponential decay of the amplitude, while figure 8 refers to a bulk mode, whose amplitude is an oscillatory function of the plane index n. The components of the amplitude of each mode on the two sublattices are opposite in phase, because of the AF nature of the system.

The dispersion curves show a strict analogy with those found in a semi-infinite system [15, 16], the only difference being a continuum in the semi-infinite system for the bulk modes. In fact, for the surface modes we have numerical evidence (analytical for $n = 2$) that the gap is given by

$$E(k_\parallel = 0) = [H_A H_E + H_A^2]^{1/2} \tag{24}$$

which equals the one found for the semi-infinite system.

Finally, for $k_z = \pi$ and/or $k_y = \pi$ only two distinct frequencies exist. All the modes are localized exactly on a plane: the two outer ones for the lower energy and an inner one for the $(N - 2)$ modes of higher energy. A similar result was also obtained for different wave vectors $k_\parallel$ in ferromagnetic films [3]. This happens because, at the boundaries of the 2D Brillouin zone, adjacent planes are exactly decoupled:

$$\gamma(k_\parallel) = \tfrac{1}{2}\cos(k_z/2)\cos(k_y/2) = 0 \qquad \text{if } k_z = \pm\pi \text{ or } k_y = \pm\pi \tag{25}$$

so that the dynamical matrix becomes diagonal.

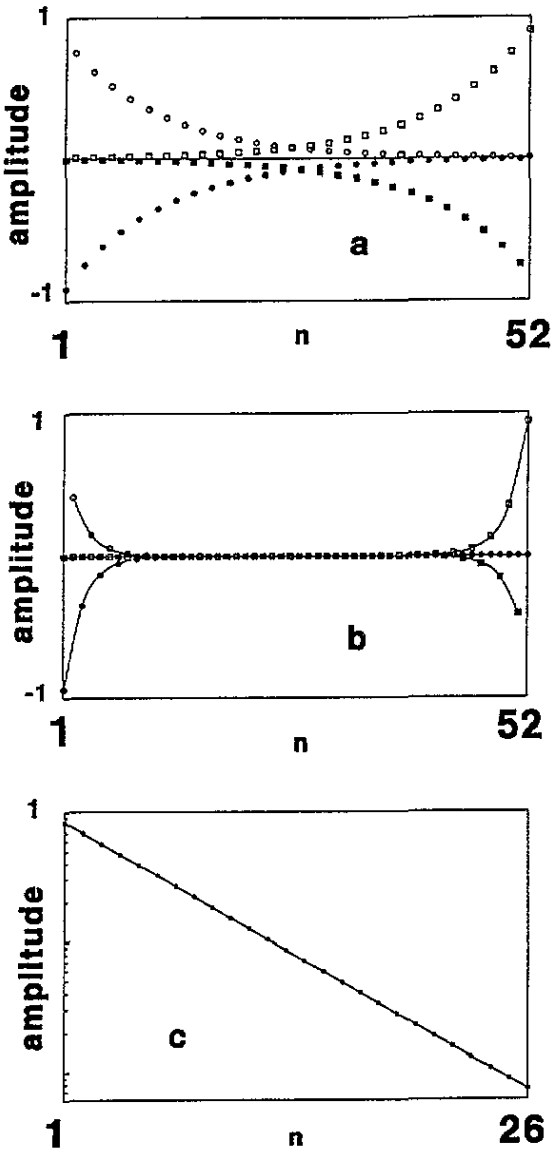

Figure 7. (a) Amplitude on both the sublattices of the eigenvectors associated with the two surface modes for $k_{\parallel} = 0$. The full (open) circles refer to the A (B) sublattice component of the eigenvector associated with the mode localized on the first plane. The full (open) squares refer to the A (B) sublattice component of the eigenvector associated with the mode localized on the last plane. (b) The same as (a) for $k_{\parallel} = (\pi/4, \pi/4)$. The solid lines provide a guide for the eyes. (c) The log plot of the amplitude on the A sublattice of the surface mode localized on the first plane for $k_{\parallel} = 0$.

• $0 < H < H_S$, $J_0 = 0$. The application of a field breaks the equivalence of the two sublattices and removes the degeneration. This is clearly seen in figure 9 where the dispersion curves are reported. It must be stressed that it is possible to speak of the same modes because in the present collinear ground state the field modifies only the diagonal elements of the matrix T, and consequently the eigenvectors are not modified. The removal

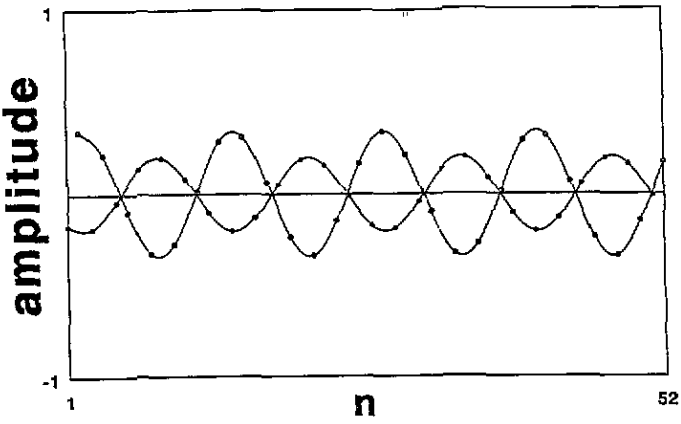

Figure 8. Amplitude on both the sublattices of the eigenvector associated with a bulk mode for $k_{\parallel} = 0$.

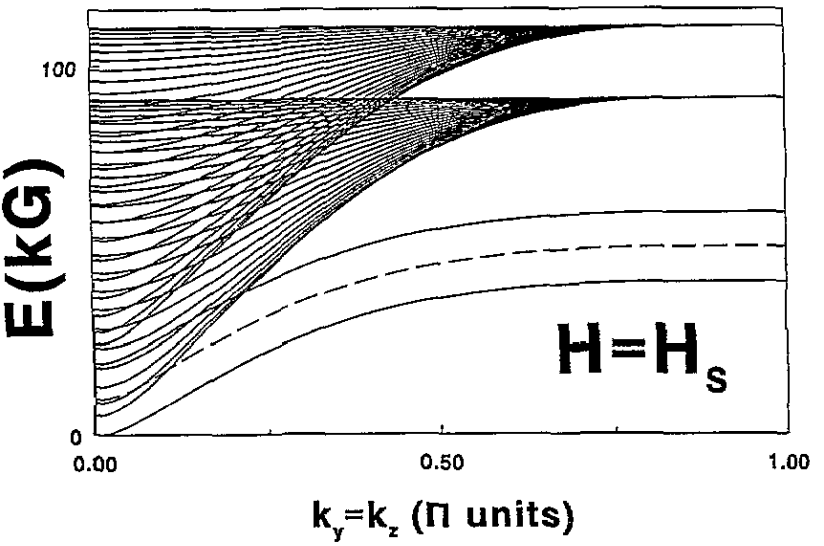

Figure 9. The energy spectrum for a $N = 52$-plane film for $H = H_S$. The field has removed the degeneracy of figure 6. The frequency at $k_{\parallel} = 0$ of the surface mode relative to the surface with spins antiparallel to H goes soft. The dashed line refers to the two degenerate surface modes for $H = 0$.

of the degeneracy is particularly important for the surface modes. Their gaps become

$$\Delta_1 = [H_A H_E + H_A^2]^{1/2} - H \tag{26a}$$

$$\Delta_2 = [H_A H_E + H_A^2]^{1/2} + H \tag{26b}$$

where the sign $-$ $(+)$ refers to the mode localized on the surface with the spins antiparallel (parallel) to the field, i.e. on the first (last) plane of the system, due to the conventions we have adopted. Of course, when $H = H_S = [H_A H_E + H_A^2]^{1/2}$, we have a complete softening of the first one (just this case is reported in figure 9), which signals a change in the ground state. In fact, for this value of the field, using the method outlined in section 2, we obtain a non-uniform ground state.

It is important to note that the removal of the degeneracy of the bulk modes presents the same characteristic as the surface ones. In fact, at the Brillouin zone boundary we have still a complete localization but with different energies between the two sublattices.

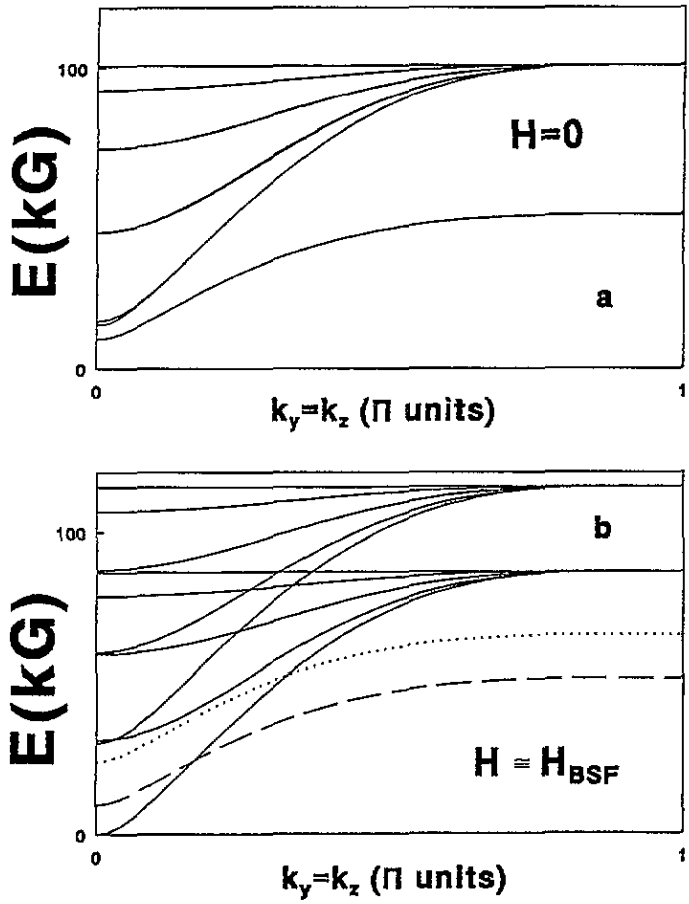

Figure 10. The energy spectrum for a $N = 53$-plane film for $H = 0$ (a) and $H \simeq H_{BSF}$ (b). Only some modes are reported. In (b) the dashed line refers to the surface modes for $H = 0$; the dotted line refers to the surface modes for $H \simeq H_{BSF}$. It is evident that it is a bulk mode that shows a complete softening for $H \simeq H_{BSF}$.

We conclude this section by noting that the different behaviour for the two surface mode gaps given by equations (26) summarizes the results obtained for the semi-infinite system [15, 16]. In the latter case we have only one surface mode, which shows a full softening for $H = H_S$ only if the spins on the surface plane are antiparallel to the field. Otherwise, when the surface spins are parallel to H, we have a full softening of the lowest-energy bulk mode for $H = H_{BSF}$. A further confirmation of this behaviour is obtained considering a film with an odd number of planes. Assuming that the surface spins are parallel to H we see from figure 10 that in this case it is a bulk mode which shows a complete softening for $H \simeq H_{BSF}$, as it was already observed by LePage and Camley [20].

• $H < H_S$, $J_0 \neq 0$. The excitation spectrum pertinent to the case of the superlattices composed by ferromagnetic films antiferromagnetically coupled is reported in figure 11, where we have assumed $J_0/J = 20$. In particular, in order to emphasize the effect of the antiferromagnetic coupling, in figure 11 we have reported the energy E' obtained from the actual energy E of the system by the subtraction of the quantity $z_0 J_0 S(1 - \gamma_0(k_\parallel))$, which represents the energy excitation of a ferromagnetic plane. We can observe that the spectrum

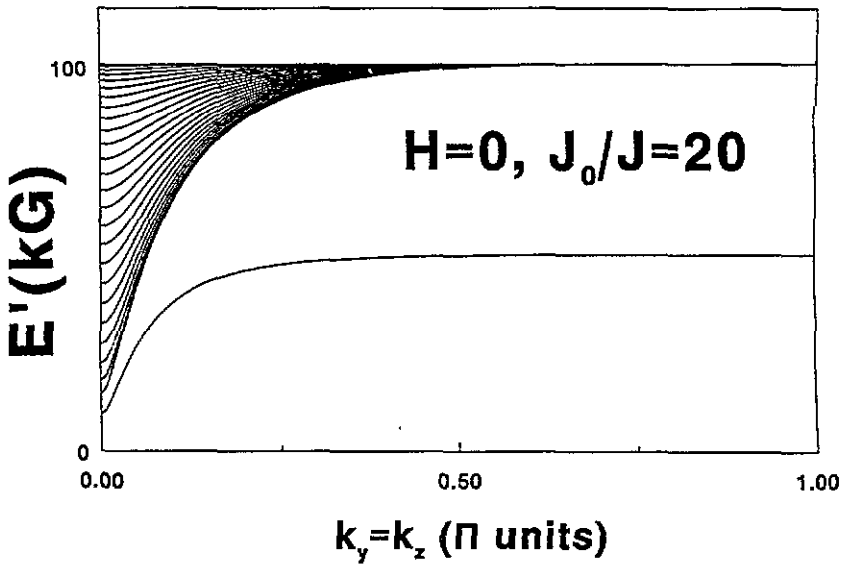

Figure 11. The energy spectrum for a superlattice composed by $N = 52$ ferromagnetic films antiferromagnetically coupled for $H = 0$ and $J_0/J = 20$, after the subtraction of the energy of a ferromagnetic plane $z_0 J_0 S(1 - \gamma_0(k_\parallel))$.

shows the same behaviour found for $J_0 = 0$ (see figure 6): the eigenvalues at the Brillouin zone centre (i.e. for $k_\parallel = 0$) and at the Brillouin zone boundary (i.e. for $k_y = \pi$ and/or $k_z = \pi$) have exactly the same value as in the previous case, but in the present case we have a stronger dispersion at low wavevectors followed by a large $k_\parallel$-region where the energy is substantially constant. In order to gain some information about the $k_\parallel$-dependence of the excitation energies let us consider a simple bilayer in the absence of anisotropy and magnetic field. The energy E' is given by

$$E'(k_\parallel) = -z_0 J_0 S(1 - \gamma_0(k_\parallel)) + z_0 J_0 S[(1 - \gamma_0(k_\parallel))^2 + (zJ_{AF}/2z_0 J_0)^2(1 - 4\gamma_0^2(k_\parallel)) + (zJ_{AF}/z_0 J_0)(1 - \gamma_0(k_\parallel))]^{\frac{1}{2}}. \tag{27}$$

For $k_y = k_z = k \to 0$, the previous equation gives $E'(k_\parallel) = \sqrt{(z_0 J_0 z J_{AF} S^2/2)}k$. From the comparison with the equivalent result obtained for $J_0 = 0$, $E(k_\parallel) = (zJ_{AF}S/2\sqrt{2})k$, one can see that the presence of ferromagnetic coupling determines a steeper growth of the energy with the wavevector. The similarity with the $J_0 = 0$ situation is confirmed by the analysis of the eigenvectors: the same character and evolution as in the antiferromagnetic film case, shifted for lower values of the wavevector, are found.

5. Elementary excitations: non-uniform ground state

In section 2 we have determined the non-uniform ground state of the system when $H > H_S$. Introducing in the T matrix (15) the thus-obtained angles, the eigenvalues and eigenvectors can be determined. In figures 12 and 13 the dispersion curves for a film with $N = 52$ and for two different fields, $H_S < H < H_{BSF}$ and $H > H_{BSF}$, and for $J_0 = 0$, are shown. We label the various modes with an index $m = 1, \ldots, N$ from the lowest one in energy to the highest one, for each value of $k_\parallel$. We can observe some general characteristics.

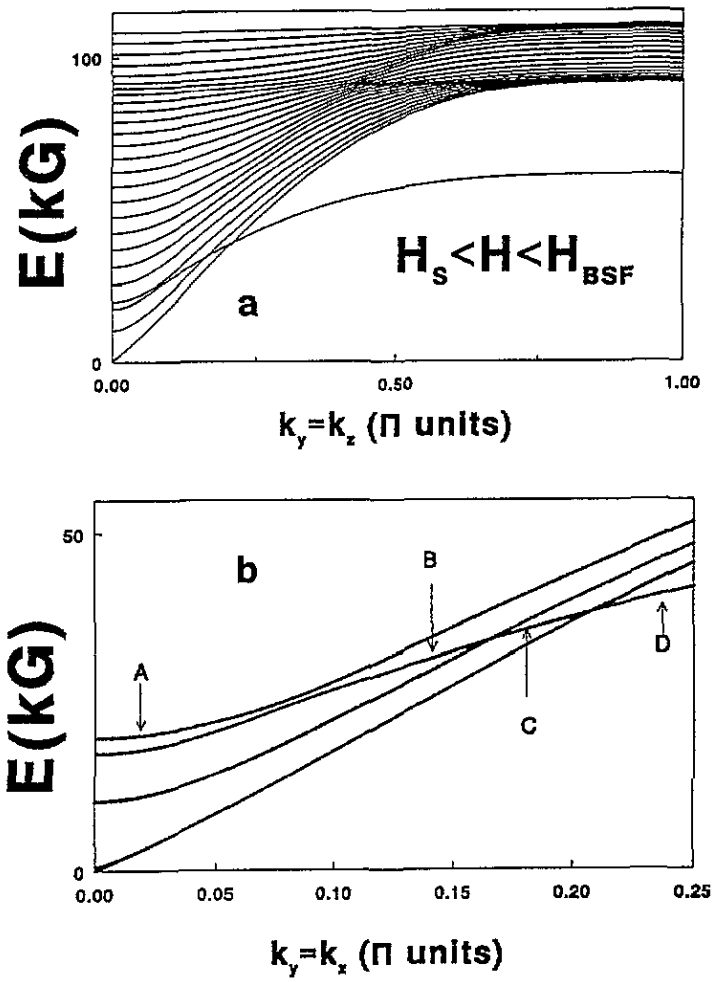

Figure 12. (a) The energy spectrum for $H = 10$ kG assuming the non-collinear ground state of figure 3. (b) Details of (a) showing the hybridization phenomenon of the lowest eight modes. The localized eigenvectors corresponding to the modes indicated with A–D are shown in figure 14.

• Degeneracy is absent, even though the energy difference between two modes is so small that it is not resolved at the scale of figures 12, 13.

• Owing to the rotational symmetry around the easy axis z the system presents a Goldstone mode and the energy vanishes linearly with $k_\parallel$. We would like to stress that the accuracy with which the correct $E = 0$ limit is obtained is a measure of the precision of the ground state calculated in section 2. Quantitatively, in order to obtain zero energy within at least six significant figures it is necessary to determine the ground state within machine double precision. The eigenvector corresponding to the Goldstone mode is reported in figure 14 where it is possible to observe the bulk character and of course the absence of nodes.

• The separation at $k_\parallel = 0$ of the two lowest-energy modes decreases on lowering of the field. In fact, decreasing the field to H'_S, the non-uniform configuration becomes unstable and the system undergoes a transition to the collinear ground state. This transition is signalled by the full softening for $k_\parallel = 0$ of the second mode.

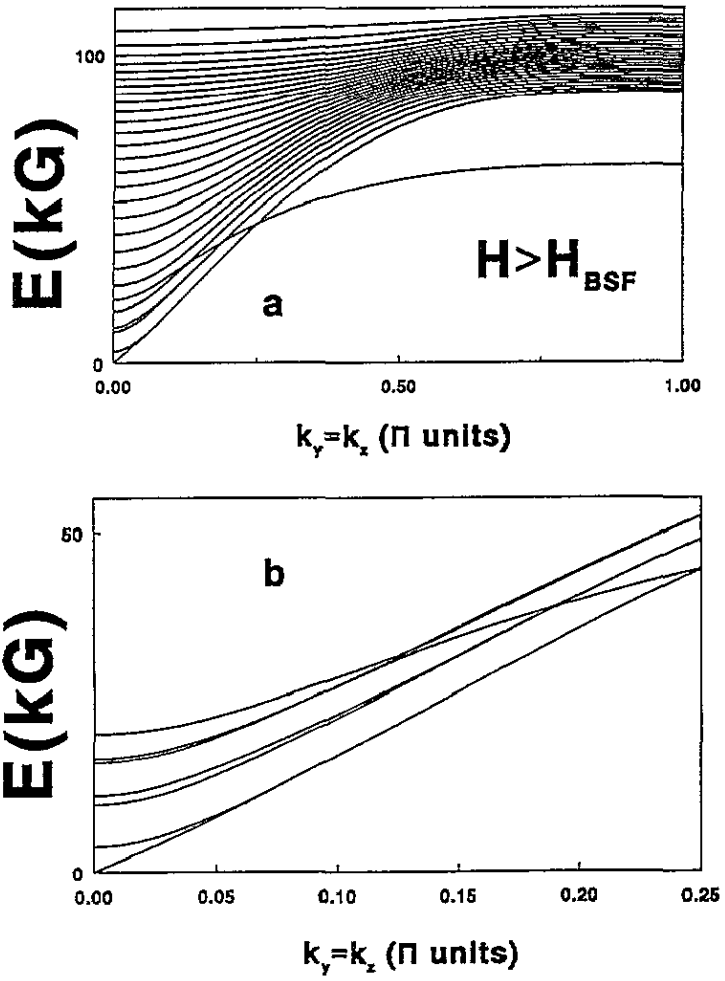

Figure 13. (a) The energy spectrum for $H = 15$ kG assuming the non-collinear ground state of figure 5. (b) Details of (a) showing the hybridization phenomenon of the lowest eight modes.

• For low values of $k_{\parallel}$ the lowest-energy modes have a bulk character, while the localized surface modes have a higher energy (see figures 12(b), 15). Increasing the wavevector, we observe successive hybridizations, so that for sufficiently high wavevectors $k_{\parallel}$ the localized surface modes do have the lowest energy. In contrast to the collinear case, each of the two surface modes is localized close to *both* the surfaces: the $S^{+}_{A(B)}$ component of the associated eigenvector close to the first (last) plane, and the $S^{-}_{A(B)}$ component close to the last (first) plane. In figure 15 the eigenvectors associated with the surface modes are reported for different values of $k_{\parallel}$. We can observe from figure 15 that for a very low value of the wavevector the surface modes present a low degree of localization; this is due to the substantial isotropization of the spin space induced by the external field for $H \simeq H_{BSF}$, so that the localization is present in a clear way only for higher values of $k_{\parallel}$ (remember that in the collinear phase the localization appears only for $k_{\parallel} \neq 0$ if $H_A = 0$, see section 4). In figure 16 the evolution of the eigenvectors of the four lowest modes involved in the last hybridization (C/D in figure 12(b)) is shown. For greater values of the wavevector, the

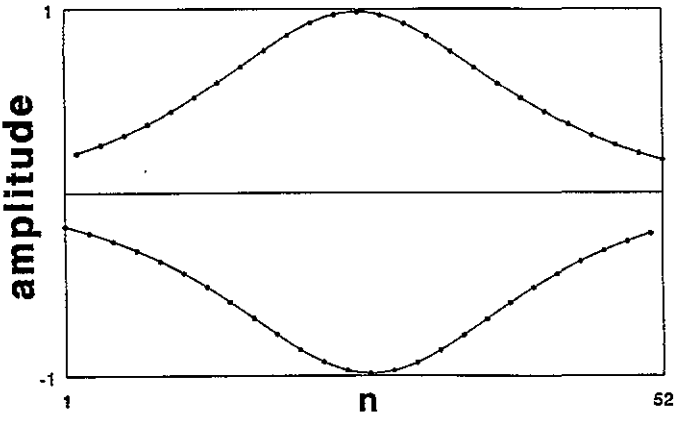

Figure 14. The $S^{\pm}$ components (indistinguishable) on both the sublattices of the eigenvector corresponding to the Goldstone mode for $H =$ 10 kG.

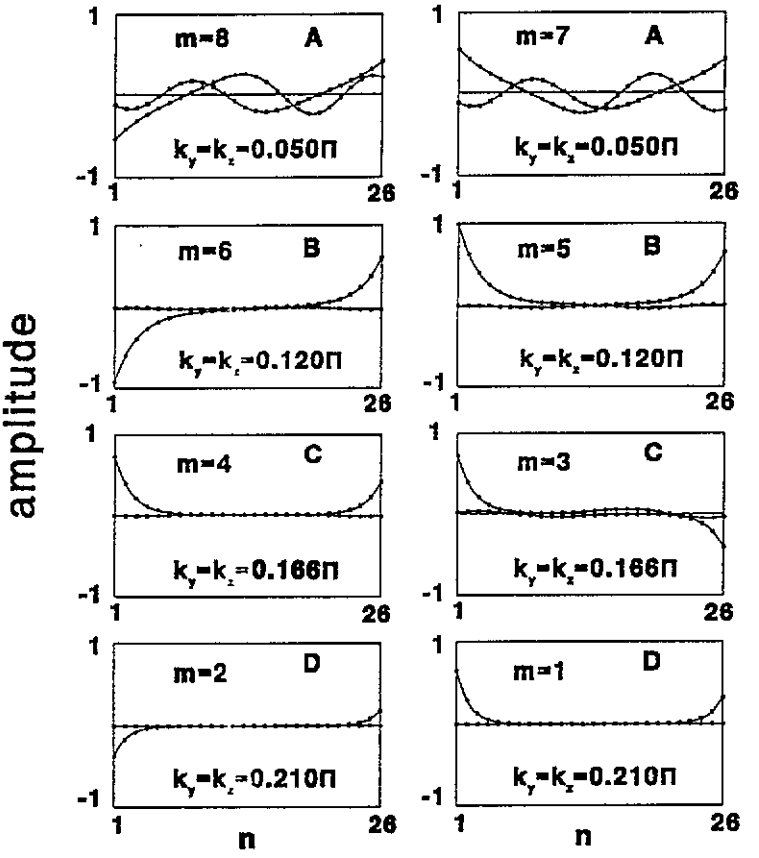

Figure 15. Amplitude of the localized eigenvectors for $H = 10$ kG and different values of $k_{\parallel}$. The circles (squares) refer to the S^{+} (S^{-}) components on the A sublattice of the eighth and seventh mode in A, of the sixth and fifth mode in B, of the fourth and third mode in C, and finally of the second and first mode in D.

eigenvectors relative to the two lowest modes always maintain a localized character.

• Finally, from the comparison of the dispersion curves shown in figures 12(a), 13(a), we can note a difference between the $H_S < H < H_{BSF}$ case and the $H > H_{BSF}$ one. In

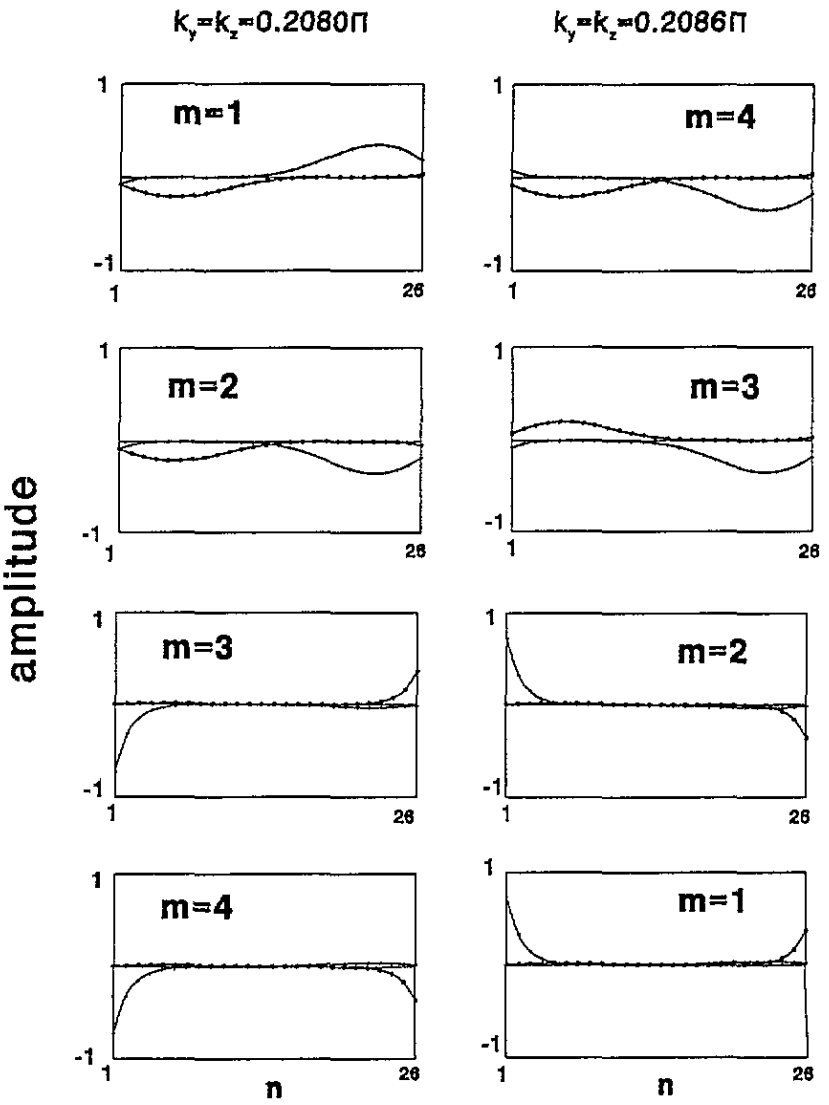

Figure 16. The S^+ (crosses) and S^- (circles) components on the A sublattice of the first ($m = 1$), second ($m = 2$), third ($m = 3$), and fourth ($m = 4$) mode for $k_\parallel = (0.2080\pi, 0.2080\pi)$, and for $k_\parallel = (0.2086\pi, 0.2086\pi)$, for $H = 10$ kG. The eigenvectors corresponding to the two lowest-energy modes acquire a localized character after this last hybridization.

the first case, the dispersion curves nearly condense at two different values at the Brillouin zone boundary. This is reminiscent of the collinear behaviour (see figure 9), and it is a consequence of the nearly parallel or antiparallel orientation with respect to the field of a large number of the spins in this regime, though the configuration is non-uniform (see section 2 and figure 4). In contrast, for $H > H_{BSF}$, the orientation of a large number of the spins is close to the bulk spin flop configuration (i.e. almost perpendicular to the field) and consequently the dispersion curves do not present such a behaviour.

Again, for $J_0 \neq 0$ (see figure 17), the only significant difference from the antiferromagnetic film case is the stronger dispersion of the energy spectrum for low value

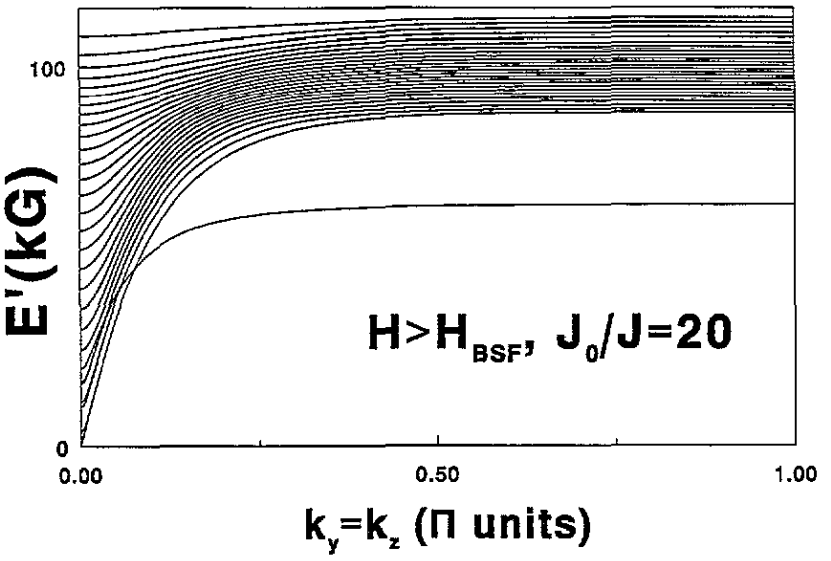

Figure 17. The energy spectrum for a superlattice composed by $N = 52$ ferromagnetic films antiferromagnetically coupled for $H = 15$ kG and $J_0/J = 20$, after the subtraction of the energy of a ferromagnetic plane $z_0 J_0 S(1 - \gamma_0(k_\parallel))$, assuming the non-collinear ground state configuration of figure 5.

of the wavevector $k_\parallel$, as already discussed in the collinear ground state situation.

In our calculation we have neglected the dipolar interaction [21,27]. This fact does not present any consequence on the ground state, if—as we have assumed—the easy axis lies in the film plane. On the contrary the dispersion curves are modified by the dipolar interaction since the rotational invariance is not present, and therefore a Goldstone mode is absent. However, since the dipolar energy has the same order of magnitude as the anisotropy, the magnetostatic region is confined to very small $k_\parallel$. For this reason, the hybridization between the lowest modes should not be modified.

6. Conclusions

In this paper we have studied the elementary excitations of a uniaxial antiferromagnet with a magnetic field along the easy axis. The absence of translational invariance in addition to the presence of competitive interactions (magnetic field and antiferromagnetic exchange) implies, for H greater than a critical field, a non-uniform ground state, in the sense that the surface order is different from the bulk one. For a film with an even number of planes this surface reconstruction is obtained for $H > H_S \simeq \sqrt{H_E H_A}$ and it is announced by a full softening of a surface mode. In the odd case we have instead a phase transition only for $H > H_{BSF} \simeq \sqrt{2H_E H_A}$, as in the translationally invariant infinitely extended system, with a full softening of a bulk mode [20]. The consequent non-uniform ground states are obtained with high precision and the relative excitation spectrum and eigenvectors are calculated, too. We showed the localized surface modes are the most strongly influenced by the non-uniformity of the ground state, as argued in the introduction. In particular, we showed that a hybridization phenomenon for many modes occurs, and that the localized surface modes become the lowest-energy ones on increasing of the wavevector, by means of successive hybridization.

Furthermore, in order to apply our treatment to ferromagnetic multilayers antiferromagnetically coupled, we took into account a strong intralayer ferromagnetic interaction and we discussed its effects both on the excitation spectrum and the eigenfunctions. Our result can be relevant to the study of the giant magnetoresistance phenomenon [10] displayed by these systems. First, the correct non-uniform ground state obtained for $H > H_S$ is fundamental in order to reproduce the field dependence of the resistance for H lower than the saturation value for which a ferromagnetic order is reached, and secondly, the calculation of the spectrum in the whole Brillouin zone is very important in order to obtain the temperature dependence of the resistance itself.

Appendix. Explicit form of the matrices T^{ij}

$$T^{11}_{n,n'} = \Big[+H\cos\theta_{2n-1} + 2KS\cos^2\theta_{2n-1} - KS\sin^2\theta_{2n-1} - \frac{zSJ}{2}(\cos(\theta_{2n} - \theta_{2n-1}) + (1-\delta_{1,n})\cos(\theta_{2n-2} - \theta_{2n-1})) + z_0 J_0 S(1 - \gamma_0(k_\parallel)) \Big] \delta_{n,n'} \tag{A1a}$$

$$T^{22}_{n,n'} = \Big[+H\cos\theta_{2n} + 2KS\cos^2\theta_{2n} - KS\sin^2\theta_{2n-1} - \frac{zSJ}{2}(\cos(\theta_{2n} - \theta_{2n-1}) + (1-\delta_{n,\frac{N}{2}})\cos(\theta_{2n+1} - \theta_{2n})) + z_0 J_0 S(1 - \gamma_0(k_\parallel)) \Big] \delta_{n,n'} \tag{A1b}$$

$$T^{13}_{n,n'} = (KS\sin^2\theta_{2n-1})\delta_{n,n'} \tag{A1c}$$

$$T^{24}_{n,n'} = (KS\sin^2\theta_{2n})\delta_{n,n'} \tag{A1d}$$

$$T^{12}_{n,n'} = \frac{zSJ}{2}\gamma(k_\parallel)(1 - \cos(\theta_{2n-1} - \theta_{2n'}))\delta_{2n-1+\delta_n,2n'} \tag{A1e}$$

$$T^{14}_{n,n'} = \frac{zSJ}{2}\gamma(k_\parallel)(1 + \cos(\theta_{2n-1} - \theta_{2n'}))\delta_{2n-1+\delta_n,2n'} \tag{A1f}$$

where

$$\gamma(k_\parallel) = \frac{1}{z}\sum_{\delta_\parallel}\exp(-\mathrm{i}k_\parallel\cdot\delta_\parallel) = \tfrac{1}{2}\cos(k_z/2)\cos(k_y/2) \tag{A2a}$$

$$\gamma_0(k_\parallel) = \frac{1}{z_0}\sum_{\delta_0}\exp(-\mathrm{i}k_\parallel\cdot\delta_0) = \tfrac{1}{2}(\cos(k_z) + \cos(k_y)). \tag{A2b}$$

Finally, we observe that in order to take kinematic consistency into account [30], it is sufficient to replace the anisotropy constant K by the effective value $K(1 - 1/2S)$ both in the ground state equations and in the dynamical matrix T.

References

[1] Rado G T 1957 *Bull. Am. Phys. Soc.* **2** 127
[2] Mills D L and Maradudin A A 1967 *J. Phys. Chem.* **28** 1855
[3] Politi P, Pini M G and Rettori A 1992 *Phys. Rev.* B **46** 8312
[4] Erickson R P and Mills D L 1991 *Phys. Rev.* B **33** 10715
[5] *Nörtemann* F C, *Stamps* R L, *Carriço* A S *and Camley* R E 1992 *Phys. Rev.* B **46** 10847
[6] Wang R W, Mills D L, Fullerton E E, Mattson J E and Bader S D 1994 *Phys. Rev. Lett.* **72** 920
[7] Trallori L, Politi P, Rettori A, Pini M G and Villain J 1994 *Phys. Rev. Lett.* **72** 1925
[8] Borchers J A, Carey M J, Erwin R W, Majkrzak C F and Berkowitz A E 1993 *Phys. Rev. Lett.* **70** 1878
[9] Ramos C A, Lederman D, King A R and Jaccarino V 1990 *Phys. Rev. Lett.* **65** 2913

[10] Baibich M N, Broto J M, Fert A, Nguyen Van Dan F, Petroff F, Etienne P, Creuzet G, Friederich A and Chazelas J 1988 *Phys. Rev. Lett.* **61** 2472
[11] Barthélémy A, Fert A, Morel R and Steren L 1994 *Phys. World* November
[12] Tang H, Walker T G, Scott J C, Chappert C, Hopster H, Pang A W, Dessau D S and Pappas D P 1993 *Phys. Rev. Lett.* **71** 444
[13] Néel L 1936 *Ann. Phys., Paris* **5** 232
[14] Anderson F B and Callen H B 1964 *Phys. Rev.* A **136** 1068
[15] Mills D L and Saslow W M 1968 *Phys. Rev.* **171** 488; erratum 1968 *Phys. Rev.* **176** 760
[16] De Wames R E and Wolfram T 1969 *Phys. Rev.* **185** 752
[17] Mills D L 1968 *Phys. Rev. Lett.* **20** 18
[18] Keffer F and Chow H 1973 *Phys. Rev. Lett.* **31** 1061
[19] Trallori L, Politi P, Rettori A, Pini M G and Villain J 1995 *Phys. Rev. Lett.* submitted
[20] LePage J G and Camley R E 1990 *Phys. Rev. Lett.* **65** 1152
[21] Wang R W and Mills D L 1994 *Phys. Rev.* B **50** 3931
[22] Carriço A S, Camley R E and Stamps R L 1994 *Phys. Rev.* B **50** 13 453
[23] Aubry S 1979 *Solitons and Condensed Matter Physics* ed A R Bishop and T Schneider (New York: Springer)
[24] Bak P 1981 *Phys. Rev. Lett.* **46** 791
Jensen M H and Bak P 1983 *Phys. Rev.* B **27** 6853
[25] Belorov P I, Beloshapkin V V, Zaslavskiĭ G M and Tret'yakov A G 1984 *Zh. Eksp. Teor. Fiz.* **87** 310 (Engl. Transl. 1984 *Sov. Phys.–JETP* **60** 180)
[26] Pandit R and Wortis M 1982 *Phys. Rev.* B **25** 3226
[27] Nörtemann F C, Stamps R L and Camley R E 1993 *Phys. Rev.* B **47** 11 910
[28] Camley R E and Stamps R L 1993 *J. Phys.: Condens. Matter* **5** 3727
[29] Maleev S V 1976 *Sov Phys.–JETP* **43** 1240
[30] Balucani U, Pini M G, Rettori A and Tognetti V 1980 *J. Phys. C: Solid State Phys.* **13** 3895